

PROCEEDINGS OF SPIE

SPIEDigitalLibrary.org/conference-proceedings-of-spie

Drone-based quantum communication links

Andrew Conrad, Samantha Isaac, Roderick Cochran,
Daniel Sanchez-Rosales, Tahereh Rezaei, et al.

Andrew Conrad, Samantha Isaac, Roderick Cochran, Daniel Sanchez-Rosales, Tahereh Rezaei, Timur Javid, A. J. Schroeder, Grzegorz Golba, Daniel Gauthier, Paul Kwiat, "Drone-based quantum communication links," Proc. SPIE 12446, Quantum Computing, Communication, and Simulation III, 124460H (8 March 2023); doi: 10.1117/12.2647923

SPIE.

Event: SPIE Quantum West, 2023, San Francisco, California, United States

Drone-Based Quantum Communication Links

Andrew Conrad^a, Samantha Isaac^a, Roderick Cochran^b, Daniel Sanchez-Rosales^b, Tahereh Rezaei^a, Timur Javid^a, A.J. Schroeder^a, Grzegorz Golba^a, Daniel Gauthier^b, and Paul Kwiat^a

^aDepartment of Physics, University of Illinois at Urbana-Champaign (UIUC), 1110 W Green St. Loomis Laboratory, Urbana, IL 61801

^bDepartment of Physics, The Ohio State University, 191 W Woodruff Ave, Columbus, OH 43210

ABSTRACT

Quantum networks between mobile platforms enable secure communication, distributed quantum sensors, and distributed quantum computing. As progress towards a future quantum internet continues, connecting mobile platforms (*e.g.*, unmanned drones, smart vehicles, ships, and planes) to quantum networks remains a challenge. For instance, engineering constraints for real-world mobile platforms require low size, weight, and power (SWaP) for quantum systems. Additionally, single photons must be routed to platforms that are in motion and experience vibrations. In this effort, we discuss progress toward developing and demonstrating quantum communication links, including decoy-state quantum key distribution (QKD), between mobile drone and vehicle platforms in several configurations (drone-to-drone, drone-to-moving vehicle, and vehicle-to-vehicle). We will discuss and analyze critical subsystems including our decoy-state QKD source based on resonant cavity light emitting diodes (LED), compact optical system design, pointing, acquisition, and tracking (PAT) subsystem, single-photon detectors, field-programmable gate array-based time-tagger, and a novel time-synchronization algorithm. In addition, we present system performance including tracking performance under multiple conditions and mobile platform configurations.

Keywords: Quantum Key Distribution (QKD), Free-Space Quantum Communications, Autonomous Drones, Decoy-State QKD

1. INTRODUCTION

Autonomous drones and smart vehicles will provide many benefits for our future transportation infrastructure. As autonomous platforms are leveraged for safety-critical applications, (*e.g.*, transporting, operating near humans) the need to protect communication channels from eavesdropping and spoofing attacks is essential. Quantum techniques such as quantum key distribution (QKD) can be utilized to provide secure communication, providing improvements over classical approaches; however, significant challenges exist for deploying quantum systems on mobile platforms, due to the requisite limited size, weight, and power (SWaP) of the payload. Prior free-space QKD links have been demonstrated from satellite-to-ground,¹ using airplanes in both air-to-ground,² and ground-to-air³ configurations. In addition to QKD, entanglement distribution has been demonstrated between a flying drone and two ground stations,⁴ as well as a flying drone to ground stations via a second passive relay drone.⁵ Recently, a 7-km air-to-ground quantum link was demonstrated using a drone and a stationary ground station.⁶

Unlike prior efforts, we demonstrate mobile quantum communication links between mobile platforms without using fixed ground stations. Such capabilities are required, *e.g.*, to enable quantum links between moving cars, or drones flying above ships at sea. Developing wireless quantum communication links between mobile platforms is an important step for applying quantum resources, *e.g.*, entanglement distribution, entanglement swapping, quantum teleportation, and quantum position verification (QPV),⁷ for autonomous drone constellations, and self-driving electric vehicles. Moreover, quantum links can also be multiplexed with classical communications channels to create hybrid links.

Further author information: (Send correspondence to A.C.)

A.C.: E-mail: aconrad5@illinois.edu, <http://research.physics.illinois.edu/QI/Photonics/>

Quantum Computing, Communication, and Simulation III, edited by Philip R. Hemmer,
Alan L. Migdall, Proc. of SPIE Vol. 12446, 124460H · © 2023
SPIE · 0277-786X · doi: 10.1117/12.2647923

This paper is organized as follows. In Sec. 2 we introduce the overall system design, while in Sec. 3 we present mobile quantum network results for multiple link types: air-to-air, air-to-vehicle, and vehicle-to-vehicle. Finally, a discussion is presented in Sec. 4.

2. SYSTEM DESIGN

Our system is designed to perform air-to-air quantum communication between two drone platforms in flight and leverages prior work.⁸ We use two commercial drones manufactured by Freefly Systems (Alta 8 Pro, see Fig. 1). We employ a custom-built decoy-state⁹ QKD source in the transmitter drone (Alice) that uses attenuated resonant-cavity LEDs controlled by a field-programmable gate array (FPGA). The transmitter implements a real-time true random number generator¹⁰ to determine qubit states for transmission.

Our QKD protocol uses 3 states, encoded in the polarization degree-of-freedom (DOF); the signal states are in the L/R basis (to reduce bit errors due to potential platform rotations), and error checking is performed in the H/V basis. Since three separate resonant-cavity LED sources are utilized, the potential exists for side-channel attacks using other DOFs besides polarization (*e.g.*, spatial mode, spectrum, and temporal). Therefore, we employ a single single-mode fiber to fix the spatial mode of each channel, perform narrow-band spectral filtering to make the spectrum of each channel indistinguishable, and apply novel FPGA timing compensation to ensure that the timing of the optical pulses is indistinguishable for each channel.

Next, QKD states are transmitted through the free-space channel to the receiver drone (Bob). Active stabilization using a pointing, acquisition, and tracking (PAT) system is required because the drones experience vibrations and undergo trajectory drift in flight and uncertainty in the platform's sensed position. Our PAT system is comprised of a two-stage control system consisting of an “outer loop” that provides initial pointing, acquisition, and coarse tracking using a gimbal (Movi Pro) and Near-infrared (NIR) beacons and cameras, and an “inner loop” that provides fine and fast tracking using a fast steering mirror (FSM, LR17) and counter-propagating alignment lasers and position sensitive detectors (PSD, DL100-7 PCBA3). Control actions are performed at a rate of 50 Hz for the outer loop and 800 Hz for the inner loop.

Once the qubits are received, the quantum receiving drone performs polarization projection onto the L/R and H/V basis; basis selection is achieved using a passive 50:50 beam splitter. The output from the polarization projection is fiber-coupled into multimode fiber and directed to a 4-channel single-photon detector unit (SPCM-AQ4C) located on the Bob drone. We record detection events on a custom FPGA-based timetagger using a qubit-based synchronization approach¹¹ in post-processing to achieve time-synchronization.



Figure 1. Drone QKD system.

A significant advantage of our approach includes using modular QKD transmitter and receiver systems that are platform agnostic; see Fig. 2. There is a single mechanical connector (Toad in the hole M3 Quick Release) used to secure our quantum transmitter and receiver to the drone platform. Our quantum systems use a small dedicated power supply, and there are no shared power, communication, or control signals between the host drone platform and our quantum transmitter and receiver systems. This allows these systems to be redeployed on other platforms (*e.g.*, ground vehicles) without any hardware modifications to our systems. It is expected that modular design for quantum transceivers (reusing common building blocks, *etc.*) will enable quicker development and deployment of future mobile quantum networks.

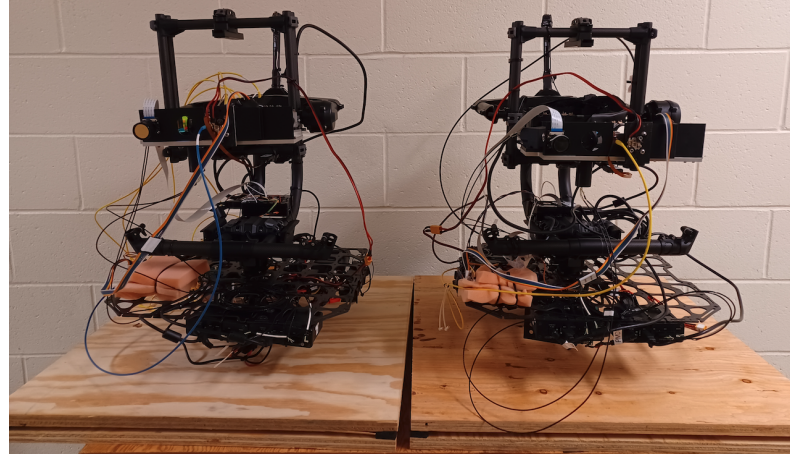


Figure 2. Our QKD payloads are modular in nature and platform agnostic.

3. RESULTS

We present results from our air-to-air QKD link using drones, air-to-car classical link, and car-to-car quantum link using the same quantum transmitter and receiver platforms in the following section.

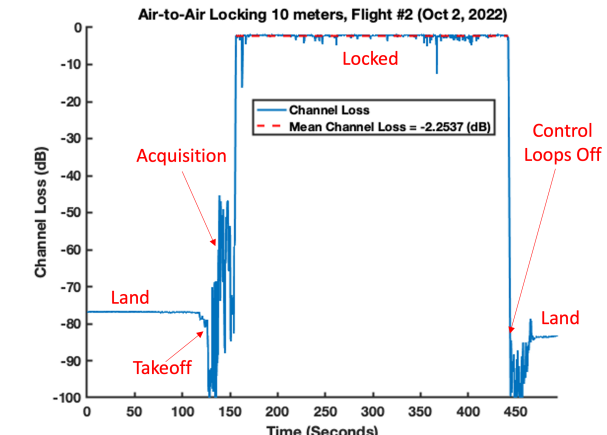
3.1 DRONE-TO-DRONE RESULTS

We performed air-to-air characterization tests of our drones in flight using a classical laser before establishing our QKD link. A photo of our drone in flight is presented in Fig. 3(a), and air-to-air classical channel loss vs. time are shown in Fig. 3(b). For this test, the airborne drones are separated by a distance of 10 m. The flight progression involves both drones starting on the ground, simultaneously taking off, and establishing a stable optical link (286 sec), before landing. Our PAT system automatically detects takeoff using a pressure sensor and begins the acquisition phase, searching for the other drone. The acquisition process continues until both PAT systems are detected and locked onto each other. Finally, when the on-board flight batteries are low, we turn off the control loops and land both drones; see Fig. 3(b). The average channel loss for this test was 2.25 dB into multimode fiber while both drones were locked onto each other. This corresponds to an average coupling efficiency of 60% from the Alice drone into multimode fiber on the Bob drone.

We demonstrated air-to-air QKD between two drones in flight over a separation distance of 10 m; see Fig. 4(a). QKD transmission as a function of time during one of the flights is shown in Fig. 4(b), which includes the raw detection events in each channel ($|R\rangle, |L\rangle, |H\rangle, |V\rangle$) as a function of time (using a 1-sec integration time). Our protocol transmits QKD states using a 5-sec on, 0.5-sec off pattern, which produces periodic dips in the raw quantum signal appearing in Fig. 4(b), useful for synchronization purposes. The quantum bit error rate (QBER) from a 0.5 sec sample from one of our flights is 2.4% in L/R basis and 2.4% in H/V basis.



(a)

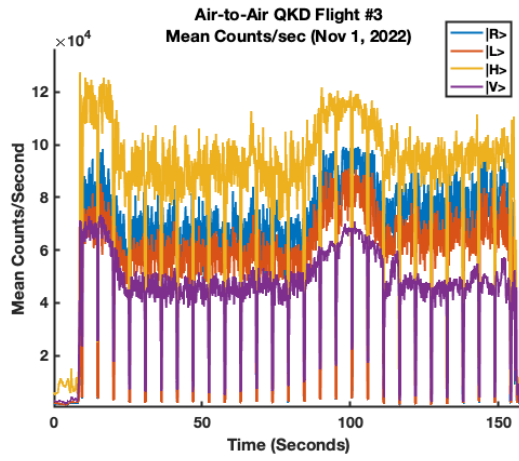


(b)

Figure 3. Air-to-Air Classical Locking. (a). Air-to-Air Setup, (b) Classical Channel Loss vs Time into multimode fiber.



(a)



(b)

Figure 4. Air-to-air drone-based QKD. (a). Air-to-air setup, and (b) temporal evolution of the QKD transmission (1-sec integration time).

3.2 DRONE-TO-VEHICLE AND VEHICLE-TO-VEHICLE RESULTS

We leveraged the modular nature of our system design and separated the receiver system from the drone and mounted it to a vehicle as shown in Fig. 6(a). An air-to-vehicle classical link is demonstrated while both the drone and vehicle are traveling parallel to each other as a speed of approximately 5 miles per hour (mph); see Fig. 6. We achieve an average of 38% coupling efficiency in the air-to-vehicle configuration into multimode fiber.

Next, we mounted both the quantum transmitter and receiver platforms in vehicles to demonstrate a quantum vehicle-to-vehicle link. The quantum transmitter (receiver) systems are placed in the rear passenger (rear driver) seats in each vehicle, as shown in Fig. 6. The quantum platforms are mounted on 2'x2' wooden bases with Sorbothane vibration dampers (see Fig. 2). We achieve an average coupling efficiency of 55% for vehicle-to-vehicle classical communication while both vehicles are traveling parallel to each other at a speed of 10 mph.

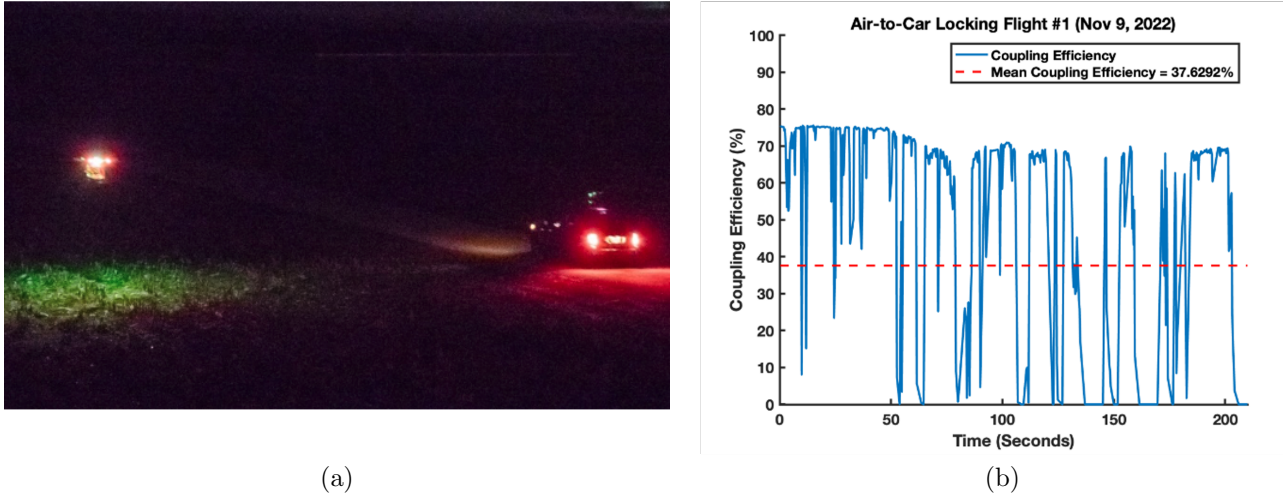


Figure 5. Air-to-car transmission. (a). Air-to-car setup. (b) Temporal evolution of the classical transmission.

We perform quantum transmission tests using laser light attenuated to the single-photon level, between two vehicles, traveling parallel to each other at 5 mph on a closed test track at the Illinois Center for Transportation (ICT); see Fig. 7. The speed of both vehicles is 5 mph. The quantum transmission is measured for three cases: using both control loops, only using the outer loop, and with the quantum source turned off (background). Better performance is achieved using both the inner and outer control loops; however, the inner control loop requires alignment lasers to operate. Our current alignment lasers for the transmitter and receiver platforms are at a wavelength of 520-nm and 705-nm, respectively, which are obviously visible to the human eye. Thus, we can only operate the alignment lasers for the inner control loop while the vehicles are on a closed test track. However, the outer control loop uses NIR beacons, centered at a wavelength of 850-nm and hence are not visible to the human eye.

Next, we performed a vehicle-to-vehicle quantum transmission test with laser light attenuated to the single-photon level using only the outer control loop (without using any alignment lasers) on a stretch of U.S. Interstate highway (I-57) into both multimode and single-mode fiber; see Fig. 8(a). Both vehicles are traveling at a speed of 70 mph (the posted speed limit) during the test. Our quantum transmitter and receiver systems are located in the back seat of each vehicle in the same configuration as shown in Fig. 6. We achieve an average signal-to-noise ratio (SNR) of 28.6 dB into multimode fiber, and 17.4 dB into single-mode fiber (Fig. 8(b) and (c) respectively) over a 60-sec-long recording session. The average signal rate is 10,465,380 counts/sec, and 97,082 counts/sec, collected into multimode and single-mode fibers, respectively. The corresponding background rate is 14,436 counts/sec for multimode fiber, and 1,733 counts/sec for single-mode fiber.

4. DISCUSSION

To the best of our knowledge, we report the first demonstration of air-to-air QKD and the first vehicle-to-vehicle quantum link on any freeway in general. Additionally, we believe this is the first demonstration of a vehicle-to-vehicle quantum link on a U.S. Interstate Highway in particular. In the future we plan to distribute entanglement in air-to-air and vehicle-to-vehicle configurations, and demonstrate entanglement-based QPV using drones and moving vehicles.

ACKNOWLEDGMENTS

This research effort is supported in part by the Department of Defense (DoD) through the National Defense Science Engineering Graduate (NDSEG) Fellowship Program, by the Air Force Research Laboratory (AFRL) through the Southwestern Ohio Council for Higher Education Fellowship Program, and by the Illinois Center for Transportation (ICT) through the Smart Transportation Infrastructure Initiative (STII). We would like to thank Alan Mitchell for taking professional photos of the drones in the field.

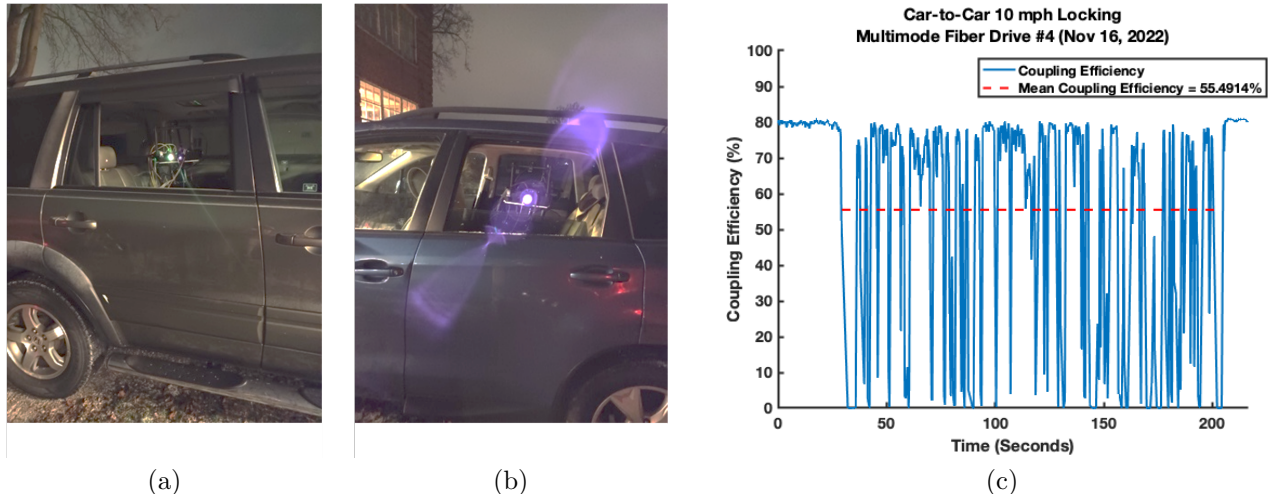


Figure 6. Car-to-car setup: (a) TX platform, (b) RX platform, and (c) classical locking results.

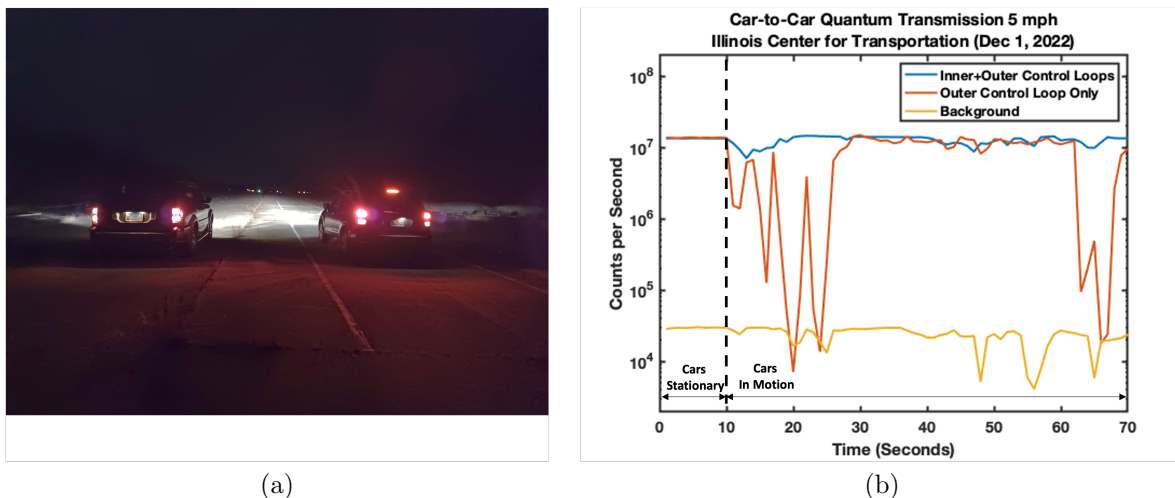
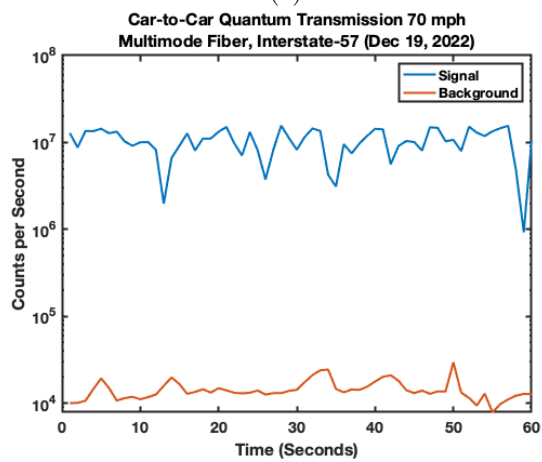


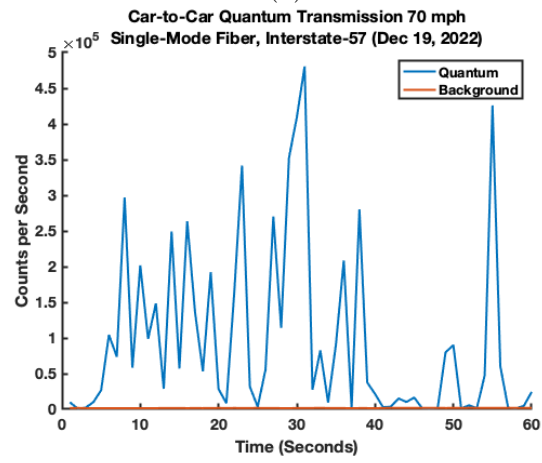
Figure 7. Vehicle-to-vehicle quantum transmission test at the Illinois Center for Transportation (ICT). (a) Setup and (b) quantum transmission results into multimode fiber.



(a)



(b)



(c)

Figure 8. U.S. Interstate Highway vehicle-to-vehicle quantum link demonstration (without using alignment lasers). (a). I-57 vehicle route (imagery courtesy Google Earth), (b) quantum transmission into multimode fiber, and (c) quantum transmission into single-mode fiber.

REFERENCES

- [1] Liao, S.-K., Cai, W.-Q., Handsteiner, J., Liu, B., Yin, J., Zhang, L., Rauch, D., Fink, M., Ren, J.-G., Liu, W.-Y., et al., “Satellite-relayed intercontinental quantum network,” *Physical review letters* **120**(3), 030501 (2018).
- [2] Nauerth, S., Moll, F., Rau, M., Horwath, J., Frick, S., Fuchs, C., and Weinfurter, H., “Air to ground quantum key distribution,” in [*Quantum Communications and Quantum Imaging X*], **8518**, 71–76, SPIE (2012).
- [3] Pugh, C. J., Kaiser, S., Bourgoin, J.-P., Jin, J., Sultana, N., Agne, S., Anisimova, E., Makarov, V., Choi, E., Higgins, B. L., et al., “Airborne demonstration of a quantum key distribution receiver payload,” *Quantum Science and Technology* **2**(2), 024009 (2017).
- [4] Liu, H.-Y., Tian, X.-H., Gu, C., Fan, P., Ni, X., Yang, R., Zhang, J.-N., Hu, M., Guo, J., Cao, X., et al., “Drone-based entanglement distribution towards mobile quantum networks,” *National science review* **7**(5), 921–928 (2020).
- [5] Liu, H.-Y., Tian, X.-H., Gu, C., Fan, P., Ni, X., Yang, R., Zhang, J.-N., Hu, M., Guo, J., Cao, X., et al., “Optical-relayed entanglement distribution using drones as mobile nodes,” *Physical Review Letters* **126**(2), 020503 (2021).
- [6] Tu, C., Shen, J., Dai, J., Zhang, L., and Wang, J., “A lower size, weight acquisition and tracking system for airborne quantum communication,” *IEEE Photonics Journal* **14**(6), 1–8 (2022).
- [7] Buhrman, H., Chandran, N., Fehr, S., Gelles, R., Goyal, V., Ostrovsky, R., and Schaffner, C., “Position-based quantum cryptography: Impossibility and constructions,” *SIAM Journal on Computing* **43**(1), 150–178 (2014).
- [8] Conrad, A., Isaac, S., Cochran, R., Sanchez-Rosales, D., Wilens, B., Gutha, A., Rezaei, T., Gauthier, D. J., and Kwiat, P., “Drone-based quantum key distribution (QKD),” in [*Free-Space Laser Communications XXXIII*], **11678**, 177–184, SPIE (2021).
- [9] Lo, H.-K., Ma, X., and Chen, K., “Decoy state quantum key distribution,” *Physical review letters* **94**(23), 230504 (2005).
- [10] Rosin, D. P., “Ultra-fast physical generation of random numbers using hybrid boolean networks,” in [*Dynamics of Complex Autonomous Boolean Networks*], 57–79, Springer (2015).
- [11] Cochran, R. D. and Gauthier, D. J., “Qubit-based clock synchronization for QKD systems using a bayesian approach,” *Entropy* **23**(8), 988 (2021).